

**EXPERIMENTAL STUDY OF A CLOSED LOOP FLAT PLATE PULSATING HEAT  
PIPE UNDER A VARYING GRAVITY FORCE**

**V. Ayel<sup>a,\*</sup>, L. Araneo<sup>b</sup>, A. Scalambra<sup>b</sup>, M. Mameli<sup>c,e</sup>, C. Romestant<sup>a</sup>, A. Piteau<sup>a</sup>,  
M. Marengo<sup>c,d</sup>, S. Filippeschi<sup>e</sup>, Y. Bertin<sup>a</sup>**

<sup>a</sup>Institut Pprime CNRS - ENSMA - Université de Poitiers, UPR 3346, Département Fluides,  
Thermique, Combustion, ENSMA, 1 av. Clément Ader - BP40109, 86961 Futuroscope-  
Chasseneuil Cedex, France

<sup>b</sup>Politecnico di Milano, Dipartimento di Energia, Via Lambruschini 4A, 20158 Milano, Italy

<sup>c</sup>Università di Bergamo, Dipartimento di Ingegneria e Scienze Applicate, Viale Marconi 5,  
24044 Dalmine, Italy

<sup>d</sup>University of Brighton, School of Computing, Engineering and Mathematics, Lewes Road,  
BN2 4GJ Brighton, UK

<sup>e</sup>Università di Pisa, DESTEC, Largo L. Lazzarino 2, Pisa, Italy

\* [vincent.ayel@ensma.fr](mailto:vincent.ayel@ensma.fr); Phone: +33 5 49 49 81 12; Fax: +33 5 49 49 81 01

## Abstract

---

This paper reports on an experimental study of a closed loop Flat Plate Pulsating Heat Pipe (FPPHP) tested on ground and on board of an aircraft during the 60<sup>th</sup> ESA parabolic flight campaign, during which hyper- and microgravity conditions were reproduced. The tested FPPHP consists in two brazed copper plates, at which location a continuous rectangular channel (1.6 x 1.7 mm<sup>2</sup>) with 12 bends in the evaporator is machined. The channel is filled with FC-72 as working fluid with a volumetric filling ratio of 50%. Tests have been conducted with the FPPHP positioned both horizontally and vertically (bottom-heated). The FPPHP presents an innovative design, involving the milling of grooves between the channels. Experimental results on the ground show that the thermal device can transfer more than 180 W in both inclinations, and that the horizontal operation is characterized by repeated stop-and-start phases and lower thermal performance. The FPPHP can operate under microgravity conditions and with a transient gravity force, with global thermal resistance reaching 50% and 25% of a void only-conduction plate, in horizontal and vertical orientation respectively. The temperature homogeneity remains within 10K in the evaporator section and 3K in the condenser section with thermal power transfer up to 180 W. Minimum thermal resistance of 0.12 KW<sup>-1</sup> was recorded, with its value rising as heating grew more powerful. A parabolic flight test demonstrated that the FPPHP in vertical inclination is rapidly influenced by variation of gravity field, even if, due to the novel geometry, it continues to operate under microgravity. In horizontal inclination, on the other hand, there was no observable parameter change during gravity field variations.

---

**Keywords:** Two-phase system, flat plate pulsating heat pipe, microgravity.

## NOMENCLATURE

$Bo$	Bond number
$D$	diameter, m
$FR$	filling ratio, %
$g$	gravity acceleration, $\text{ms}^{-2}$
$P$	pressure, Pa
$\dot{q}$	heat flux, $\text{Wm}^{-2}$
$\dot{Q}$	heat power, W
$R_{th}$	thermal resistance, $\text{KW}^{-1}$
$Re$	Reynolds number
$T$	temperature, K
$u$	velocity, $\text{ms}^{-1}$
$We$	Weber number

## Greek symbols

$\rho$	density, $\text{kg m}^{-3}$
$\sigma$	surface tension, $\text{Nm}^{-1}$

## Subscripts

air	ambient air
c	condenser zone
crit	critical
e	evaporator zone
h	heater, hydraulic
l	liquid
v	vapour

## 1- Introduction

Pulsating heat pipes (PHP) have been widely studied since the patent of Akachi [1] assigned them the configuration now largely adopted in many current works. A PHP can be defined as a single capillary channel bent in several turns between a heated zone and a cold source consisting of several interconnected turns. The tube is partially filled with a working fluid at the liquid/vapour saturation state, which is distributed by means of surface tension effects in the form of liquid slugs and vapour plugs. Under the effect of the heat source in a zone called evaporator, phase change phenomena occur in the form of liquid film evaporation or flow boiling. On the other hand, condensation occurs in the zone called condenser, which is in contact with the cold source. Complex flow patterns ranging from slug flow to annular flow are initiated in adjacent tubes by local pressure instabilities, and they have effects on the total heat flux transferred by the PHP from the heated to the cooled end [2-4].

When the flow patterns are considered in conjunction with related heat transfers, many parameters have a direct influence on PHP operation [5,6]; while the most important is obviously the channel internal diameter that allows liquid/vapour phase division into liquid slugs and vapour plugs separated by menisci [6,7], other parameters deserve mention: number of turns [8], PHP length, filling ratio, the physical properties of the working fluid or, indirectly, the cold source temperature [6,9], heat power applied or heat flux, the inclination with respect to gravity [3,9,10] and the closure or not of the overall loop [11,12]. Among the above-mentioned parameters, orientation is known to strongly affect the performances of such systems by the effect of gravity on fluid momentum; Charoensawan et al. [6] pointed out that the number of turns also affects performances at the level of internal temporal and spatial dynamic pressure perturbations. The direction of the gravity vector with respect to the 3D symmetry axis of a PHP influences not only the thermo-hydraulics of two-phase flow inside the device, but also thermal performances: a PHP always shows better operation in vertical bottom heated mode than in horizontal position, that is to say with the gravity vector oriented in the same direction or perpendicularly to the channels respectively. However, Yang et al. [8] have shown that with a sufficient number of turns and a small tube diameter, a PHP proves to be practically independent of its orientation. This last point is of particular interest in this study, since pulsating heat pipes not only remain suitable as highly efficient passive heat transfer devices for ground applications, but also show promise for space applications.

The present study can be considered as a continuation of the study previously conducted by Mameli et al. [13], in which the authors carried out an experimental

investigation on a tube CLPHP tested both on the ground and under micro/hyper gravity conditions during the 58<sup>th</sup> ESA Parabolic Flight Campaign. The PHP consisted in a copper tube with an internal diameter of 1.1 mm (just under the critical diameter for FC-72, calculated with the static criterion based on the Bond Number at 1g and 20°C:  $D_{crit} = 2(g(\rho_l - \rho_v)/\sigma)^{1/2} \approx 1.68$  mm), bent into a planar serpentine, for a total of 16 U-turns in the evaporator zone. Tests during the parabolic flights showed that the vertical operation was affected by hyper- or micro-gravity phases, the first of them slightly assisting the flow motion, and the second one leading to a sudden increase of temperature in the evaporator zone. This abrupt heightening was quite similar to the thermal dynamic response of vertical-to-horizontal tilt manoeuvre on ground. The horizontal operation does not seem to be affected by variations in the gravity field.

Gu et al. [14] have experimented two flat plate aluminum PHP models (250 x 60 x 2.2 mm outer dimensions) during parabolic flights. The PHP was filled with R114 as working fluid with filling ratio of approximately 50-60%. The single continuous channel, engraved on the bottom plate, had a cross section of 1 x 1 mm<sup>2</sup> and was laid out with 48 turns at both ends of the closed loop. Their specificity consists in the configuration of hot (55 x 16 mm<sup>2</sup> Kapton® heater) and cold (80 x 80 mm<sup>2</sup> fan) sources: the first was heated in the middle position and cooled at one end, while the other was heated and cooled at the two opposed ends. The authors concluded that both pulsating heat pipe models operated more effectively under reduced gravity than under normal or hyper-gravity phases. One may note that these conclusions have been confirmed only for top-heated mode data, which obviously yield less successful performance under unfavourable orientation than under micro-gravity or horizontal orientation. However, according to Gu et al. [14], a dimensional analysis based on Weber number ( $We = \rho u_i^2 D / \sigma$ , ratio between inertial and surface tension forces) has shown that PHPs can operate satisfactorily under microgravity with larger channel diameters (up to 5 mm with R114), i.e. with internal diameters that eventually impede operation on ground. They hypothesized that PHPs could apply larger channel diameters in space and transport more heat without gravity, but there was no experimental validation to confirm their hypothesis.

In this study, a Flat Plate Pulsating Heat Pipe (FPPHP) is designed and tested in order to meet a twofold objective: (i) to determine whether an evolving geometry with very similar boundary conditions as those in [10,13,14], but with a hydraulic diameter of about 1.65 mm, just below the critical one at ambient temperature for FC-72, can effectively work in

microgravity, and (ii) to optimize the FPPHP with respect to a microgravity transient environment. Aspects concerning the inner diameter optimization will be discussed in Section 2. It is essential to keep in mind two issues that may differentiate a FPPHP from a capillary tube PHP; they have already been discussed by Khandekar et al. [15] and thereafter by Yang et al. [16], Ayel et al. [17], as well as Qu et al. for micro-pulsating heat pipes [18]. On the one hand, square shape channels engraved in one plate of the FPPHP have sharp angles in the corners, acting like capillary grooves assisting the liquid flow. Capillary pumping from one side helps the liquid to flow back to the evaporator zone; on the other hand it may provoke rupture of the cross-sectional menisci, resulting in flow regime transition into an annular flow. Operating in favourable vertical inclination, the FPPHP works very effectively under capillary-assisted thermosyphon mode even for the lowest heat power levels, which is not the case for circular shaped channels [15,18]. On the other hand, due to geometry continuity, thermal spreading occurs and tends to strongly decrease transverse thermal resistance between channels, leading to lower temperature gradients in the gap between the channels. This causes homogenization of the pressure differences in the channels, which are the main driver of oscillations under slug flow, particularly in horizontal inclination. The FPPHP tested under this latter inclination consequently often shows premature dry-out [15,17]. To sum-up, with respect to capillary tube PHPs, FPPHPs work more effectively in the favourable inclination, while they may come to a complete stop when functioning in a horizontal position. For this reason, the present FPPHP presents a novel structure featuring thermal gaps between the channels, as shown below in Figure 1.

## **2- Flat plate PHP design and experimental setup**

### *2.1 Flat plate pulsating heat pipe*

The FPPHP tested was obtained from a copper plate (width: 120 mm, length: 200 mm, thickness: 2 mm) machined with a single rectangular shaped groove (1.6 x 1.7 mm<sup>2</sup>, hydraulic diameter:  $D_h \approx 1.65$  mm) forming a series of 12 U-turns in the evaporator (see Fig. 1a) covered with a second plate (see Fig. 1c) with the same dimensions and 1 mm of thickness. The flat plate PHP was designed with a channel cross section enhancing overall performance, while remaining within the outer dimensions of the capillary PHP in [13]. The PHP plate and its cover were brazed to guarantee perfect sealing and the adjacent channels were sealed off relative to one another. Further monitoring was carried out in order to avoid brazing material inside the channels.

As mentioned, in order to minimize transverse conduction between adjacent channels [15-17], separating grooves (1 x 1.6 mm<sup>2</sup> cross section except where there are screws) were engraved on the back-side of the PHP. Fig. 1b shows these grooves to be acting as thermal gaps; while in Fig. 1c a half-sectional view of the PHP is given, highlighting the channels in contact with the top plate, as well as the separating thermal gaps on the opposite lower side.

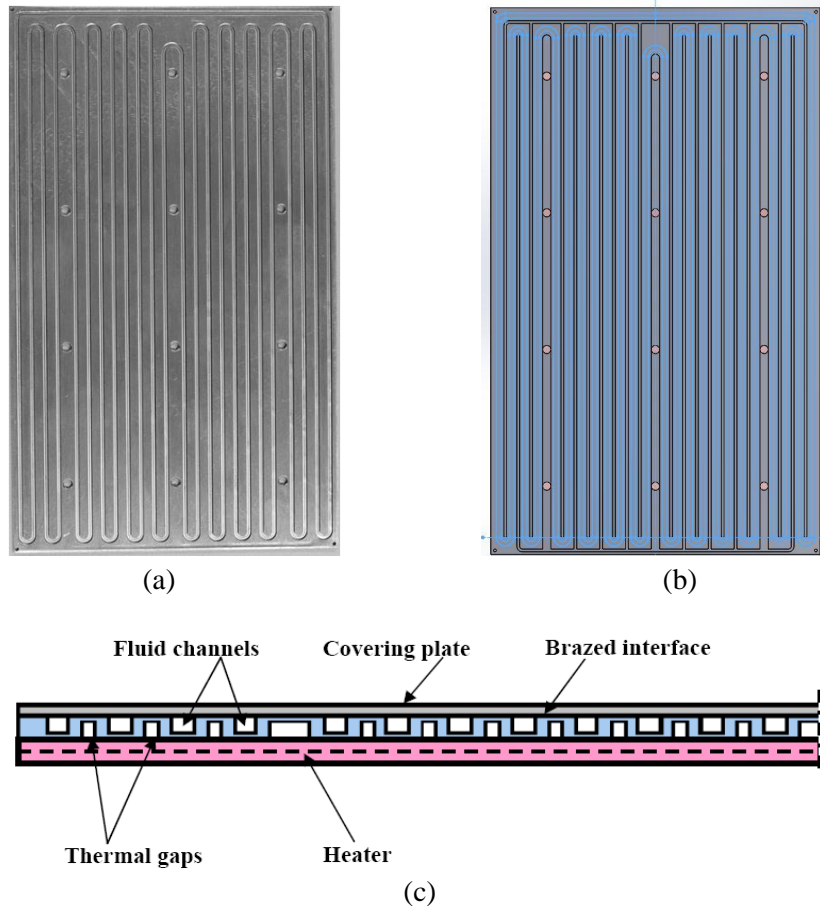


Fig. 1: View of the FPPHP: (a) photograph of the machined channel; (b) schematic view of the separating grooves on the back face and (c) half-sectional view.

As regards the cross-sectional dimensions of the channel, the existence of a slug and plug pattern in the tubes cannot be evaluated in microgravity conditions according to the critical Bond number ( $Bo_{crit} = g(\rho_l - \rho_v)D_{crit}^2/\sigma \leq 4$ ) widely used in the literature in terrestrial conditions. As argued by Mameli et al. [13] in their consideration of viscous, inertial forces and surface tension forces [19], the Weber criterion suggests, for a fluid velocity between 0.1 m.s<sup>-1</sup> (from visualizations of Gu et al. with R114 as a working fluid [20]) and 0.2 m.s<sup>-1</sup> (from visualizations of Ayel et al. with ethanol [17]) that the flow pattern should be retained as slug and plug flow in microgravity for liquid temperatures below 60°C for the present hydraulic diameter. Given that, during experiments, the temperature at the condenser never

exceeded 45°C, the flow remains slug and plug for all the tests to be presented, at least in horizontal inclination.

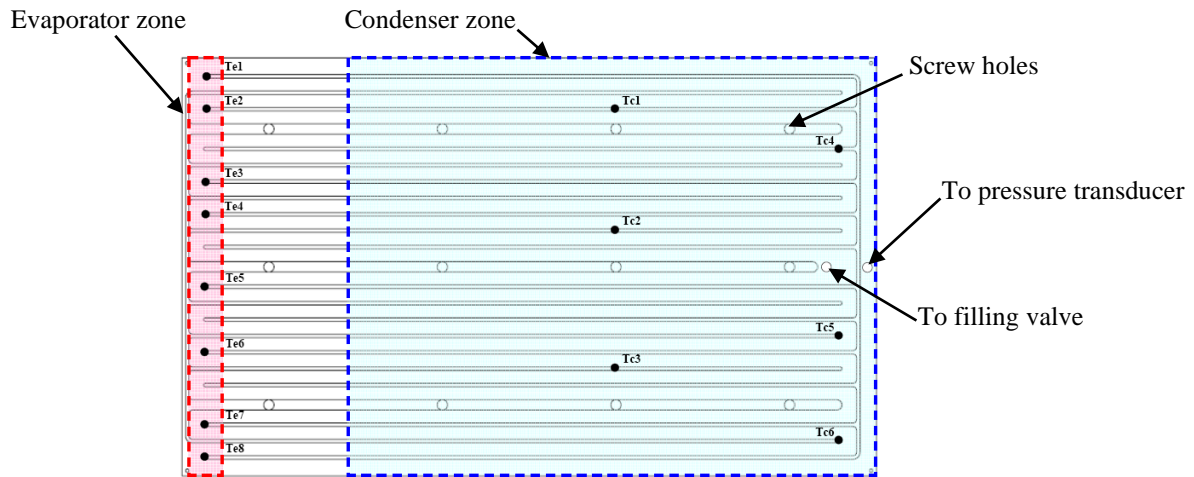


Fig. 2: Heater, cold source and sensor positions.

## 2.2 Experimental bench

The evaporator zone of the FPPHP is heated by a wire electrical heater (Thermocoax Type ZEZA10, 1 mm external diameter, electrical resistance:  $R = 3.81 \Omega$ ) embedded in a copper plate of 10 x 120 mm<sup>2</sup> dimensions and 2 mm thick by means of a serpentine groove machined on one side of the plate (see Fig. 1c and Fig. 2 for position). The latter is connected to electrical power supply (GWInstek® 3610A,  $\pm 0.2$  V) delivering heat power up to 180 W. On the opposite side, the condenser section is 165 mm long and 120 mm wide, and is embedded in an aluminum heat sink (200 x 120 mm<sup>2</sup>) cooled by means of two air fans (Sunon PMD1209PMB3-A, Fig. 3a). The PHP and the heat sink are clamped against one another with through-bolts traversing nine screw holes (Fig. 2). Both heater and heat sink interfaces are wedged with thermal grease to reduce thermal contact resistance. The heater/heat sink and PHP elements are surrounded by PTFE plates and brackets (1 mm thick, Fig. 3a) to ensure double containment assembly as prescribed by NOVSPACE security protocols, as well as partial insulation on account of the air layer thickness confined inside the heated zone. Except for the sensors, the heater and the cold source, the entire bench is the same as the one used in previous parabolic flight campaigns for tubular PHP (58<sup>th</sup> and 59<sup>th</sup> ESA Parabolic Flight Campaigns) and described in [13].



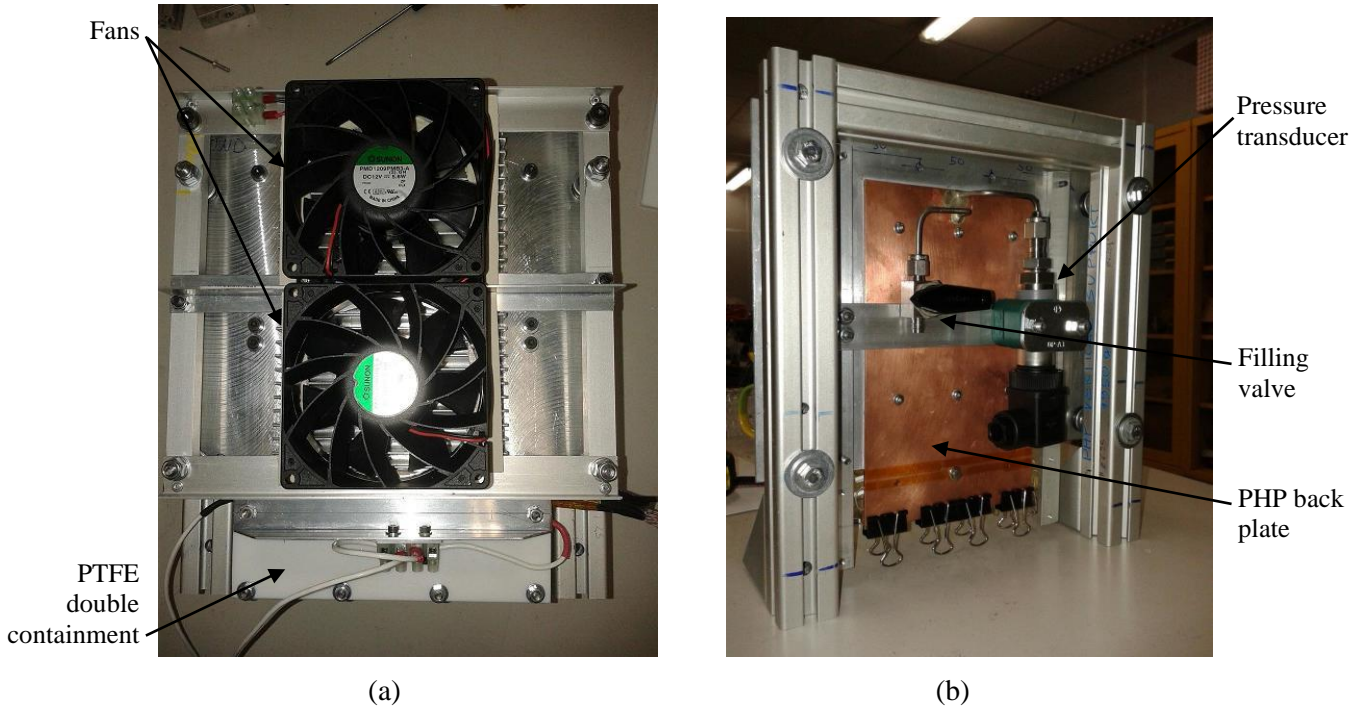


Fig. 3: FPPHP assembly: (a) heat sink with air fans system; (b) backside with pressure transducer and filling valve.

Sixteen bare T-type thermocouples of 0.5 mm (TC,  $\pm 0.5$  K) monitor the temperature of each section of the PHP: eight thermocouples were glued in eight different separating grooves on the back side of the evaporator ( $T_{e_1}$  to  $T_{e_8}$ ); six similar ones were inserted in six separating grooves on the back side of the condenser ( $T_{c_1}$  to  $T_{c_6}$ ). The position of all the sensors can be seen in Fig. 2, where it is represented by black dots. One thermocouple measures air temperature inside the heater containment ( $T_h$ ), and the last thermocouple measures air temperature upstream the fans ( $T_{air}$ ). A pressure sensor (GE PTX5076-TA-A3-CA-H0-PS, 5 bars absolute,  $\pm 200$  Pa) allows recording of local fluid pressure. A  $g$ -sensor (Dimension Engineering® DE-ACCM3D,  $\pm 0.1g$ ) located on the external confinement of the PHP is used to measure gravity level variations during the flight. The thermocouples, pressure sensor, accelerometer and power supply are all connected to a data acquisition system (NI-cRIO-9073, NI-9214 for thermocouple acquisition). All signals have been recorded at 16 Hz sampling frequency, largely satisfying the Nyquist-Shannon criterion as regards the fluctuation frequencies of the wall temperatures (of around 1 Hz maximum).

Before being filled, the PHP is evacuated by means of an ultra-high vacuum system (ASM 142, Adixen by Pfeiffer Vacuum®). The working fluid, initially contained in a tank, is degassed by heating/cooling cycles until, by means of an external valve; it achieves the right value of filling mass, which corresponds to the desired filling ratio  $FR$  at ambient temperature. After filling, the tank should be empty. The exact injected quantity of fluid is

thus deduced from the mass difference of the tank before and after filling. Lastly, the presence of non-condensable gases (NCG) is monitored by measurement of temperature and pressure of the PHP in the absence of applied heat power. Presence of NCG in the system was detectable only indirectly through verification of the pressure value, which should correspond to the saturation pressure at the given temperature. The pressure difference between the ideal saturation pressure and the measured pressure was always situated within the range of sensor accuracy; the incondensable gas content, estimated with the procedure described by Henry et al. [21] by measuring the difference between actual fluid pressure inside the PHP and its saturation pressure at ambient temperature, is consequently less than 3PPM.

The operative conditions for all the ground and microgravity tests are:

- Working fluid: FC72,  $FR \approx 50\%$  ( $\pm 2.7\%$  at ambient temperature);
- Heat power applied: from 30 W to 180 W by steps of 30 W ( $\dot{Q}$ );
- Cold source: air at ambient temperature in the plane ( $T_{air}$ );
- Orientations: horizontal and vertical (bottom heated), according to the floor of the aircraft.

### 3- Experimental results

#### 3.1 Ground tests

Before the flight campaign, the experimental device was tested on ground, for repeatability purposes, under normal gravity conditions, in vertical bottom heated mode and with horizontal orientations. One may observe in Fig. 4 and 5 some typical examples of tests of the PHP subjected to heat power levels increasing from 40 W to 150 W by steps of 10 W, for vertical and horizontal inclinations, respectively. In the case of a limited number of experiments in horizontal inclination, the PHP did not start for low heat power levels, and began to operate only when it was subjected to external movements caused randomly by the users. In vertical bottom heated mode, the applied heat power necessary for PHP start-up differed in some tests, according to the initial distribution of the fluid, as had been the case for tubular PHPs by [10]. For vertical orientation, according to Liu et al. [22], the fluid inside the FPPHP requires additional energy to trigger enough perturbations and instabilities to initiate its motion between evaporator and condenser. Nevertheless, above a given threshold value, the FPPHP always managed to function. In this paper, presentation of the results is limited to tests having worked very satisfactorily and without accidental issues, particularly for

horizontal inclination, in which the FPPHP began working even at the lowest heat power level without any external or fortuitous event. In this case, start-up behaviour of the FPPHP can be assigned to a typical first-order transient response, as described in [22].

The temperature curves are always presented in the same way; for example in Fig. 4 the temperatures at the evaporator are drawn gradually from the hottest (red curve) to the coldest (violet curve), with indications of the corresponding hottest and coldest thermocouples. It is interesting to note that during experiments the hottest thermocouple was always  $Te_5$ , located close to the middle of the evaporator zone, while the coldest was either  $Te_1$  or  $Te_8$ , i.e. the thermocouples located at the outer edges of the evaporator zone (Fig. 4, 5, 9 and 10). The same applies to the condenser thermocouples, which were drawn gradually from the hottest (dark blue curve) to the coldest (cyan curve). In this zone, and, for the following, the highest temperature was measured in the middle section, in length and width, of the condenser zone ( $Tc_2$ ), and the lowest in the upper section at the outer edge of the condenser zone ( $Tc_6$ ).

Lastly, all discussions concerning fluid behaviour inside the FPPHP are based mainly on visualization test campaigns previously performed on a glass covered flat plate copper PHP with squared channels [17,23], in conjunction with campaigns from the literature on flat plate PHPs [15,16]. It is important to keep in mind that all conclusions are provisional, and that the major issue concerning the two tested orientations is the inability of the fluid flow to function in annular flow when the PHP is tested horizontally.

First, in Fig. 4 for vertical orientation it is clear that the PHP started-up at 40 W in a purely conductive mode. At 50 W the FPPHP fluid started to move, resulting in a very sharp decrease (around 10 K) of evaporator temperatures, together with a slight increase of condenser temperatures. The thermal jump can be detected on the transient pressure black curve of Fig. 6 for the same inclination (see the peak at about 300 s). At the same time mean pressure rises from around 0.30 bar to around 0.35 bar, resulting in a pressure jump of approximately 5000 Pa. After this interval, the PHP operation is stable, with regularly increasing levels of temperature together with increasing heat power levels. The overall temperature difference in the evaporator zone increases slightly with  $\dot{Q}$ , from 2.5 K at low heat power levels to around 5 K at 150 W.

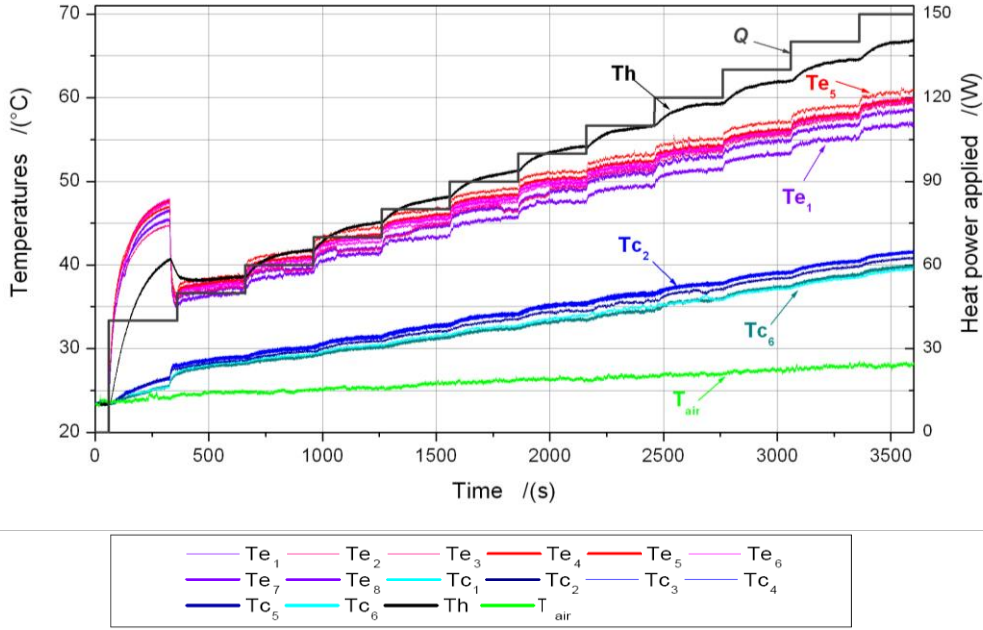


Fig. 4: Transient temperature response of the FPPHP to increasing heat power levels (ground test, vertical orientation).

Minimum and maximum temperatures are visible on Fig. 4 ( $Te_1$  and  $Te_5$ , respectively), showing that the lowest are located on the edge and the highest in the centre part of the evaporator. Two effects can help to explain the pronounced temperature difference: on the one hand, the device is clearly subjected to 2D edge effects due to heat losses to the ambient; on the other hand, the external channel bend has a longer extension inside the condensing zone (Fig. 1a). The fluid can consequently be cooled more efficiently in this zone, with a higher flow rate during the cold liquid phase.

In this study, the FPPHP works with highly stable temperature curves in most of the channels. One question is whether or not it works under an annular two-phase regime, even for the smallest values of  $\dot{Q}$ , or always with slug flow patterns. The regularity of the thermal and pressure curves and the low amplitude of temperature and pressure fluctuations could be linked to typical annular flow pattern behaviour, as has already been observed from visualizations of a FPPHP filled with ethanol in a vertical operation [17]. In this respect, it could be argued that most of the channels are filled with vapour presenting low temperature oscillations.

This consideration can be supported by the fact that, as discussed in Section 2.1, the characteristic dimension of the channels ( $1.6 \times 1.7 \text{ mm}^2$ ) suggests that the critical diameter, determined solely by the Bond number criterion of an equivalent circular tube, is exceeded for FC-72 temperature below  $35^\circ\text{C}$  [13]. If the inertial and capillary effects of the fluid flow are

taken into account, it is possible, as discussed in Section 1, that flow pattern transition from slug to annular involves the flow of liquid film along the corners of the square channels; in that case, most of the film would be collected in the evaporator.

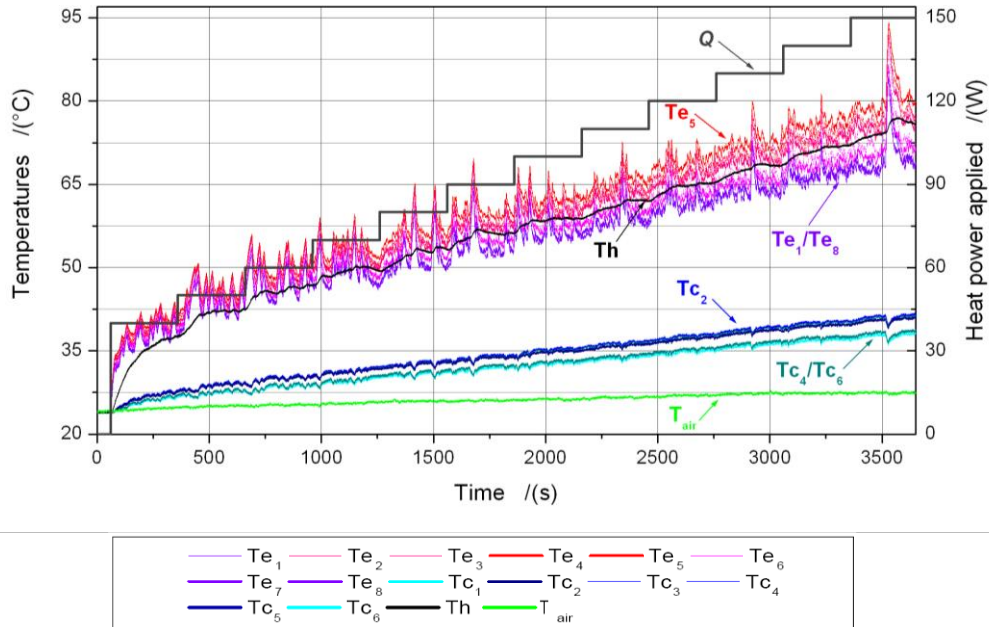


Fig. 5: Transient temperatures response of the FPPHP to increasing levels of heat power levels (ground test, horizontal orientation).

Fig. 5 and 6 show the temperatures and pressure signals for horizontal orientation. In most of the channels, the flow pattern is slug-and-plug, with vapour pushing liquid plugs from evaporator to condenser, as observed in [4]. In horizontal orientation, pressure fluctuations are much higher in amplitude and period, and much more irregular than in vertical orientation. For example, the mean amplitude of pressure fluctuations varies from around 2000 Pa to 5000 Pa, for vertical orientation (at 40 W), and from 4000 Pa to 25000 Pa for horizontal orientation (at 150 W). These fluctuations are the result of hydraulic instabilities being much larger in horizontal than in vertical position, and they show that the transfers do not occur in the same way for the two positions.

Local fluid pressure in the condenser is directly related to flow motion and shows that the horizontal mode operates with higher amplitude peaks with respect to the gravity-assisted mode. Indeed, the vertical mode is characterized by stable oscillations, while the horizontal mode reveals an alternation of short stop-overs and vigorous oscillations (Fig. 5 and 6); since the fluid is not assisted by gravity, the return of liquid slugs from the condenser to the evaporator is damped. On the other hand, vapour resides for longer periods inside the evaporator so that pressure locally increases and can push the adjacent liquid slugs with

abrupt expansions. The impulse-driven flow described above is also typical of the microgravity periods at any orientation and from the thermal point of view it leads PHP evaporator temperatures to higher levels with respect to the stable pulsating flow.

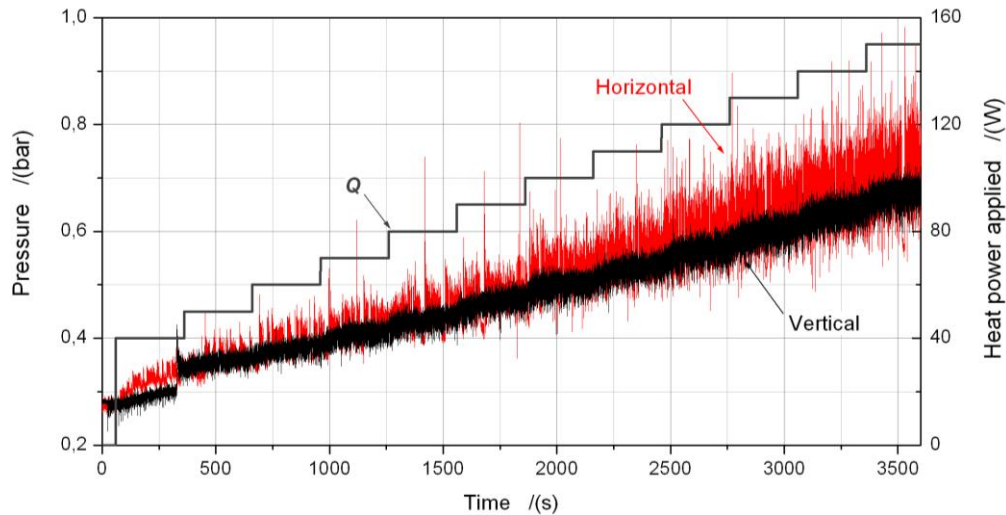


Fig. 6: Transient pressure response of the FPPHP to increasing levels of heat power levels for the two orientations on ground.

Note that, as mentioned above, the FPPHP activated at 40 W, shows very good thermal performances in this configuration. At the lowest heat power levels, the FPPHP operates horizontally in a kind of stop-and-start fluid motion, as though the fluid needed sufficient pressure difference between the evaporator and the condenser to trigger its motion. However, these irregular instabilities seem to disappear around 100 W heat power, except for some rare remaining stop-and-start phases, in which case the fluctuation levels are sufficient to cause fluid motion at any moment.

A Fast Fourier Transform analysis has been performed on pressure signals for all of the heat power steps in steady-state, on both inclinations, and it showed that no dominant frequency for this signal was detectable. Finally, the pressure curves of Fig. 6 illustrate the fact that the mean level of pressure measured in the middle part of higher channel U-turn in the condenser (see Fig. 2) gradually grows with increasing power, as do condenser temperatures.

Subsequently, tests such as those presented on Fig. 4 and 5 permitted a steady-state analysis of the FPPHP in relation to the heat power supplied. For each steady state, a special file was created involving 160 successive recordings of the data for vertical orientation, and no less than 1600 successive recordings for horizontal inclination, due to the higher level of instabilities, so that evaporator and condenser temperatures could be averaged as functions of

$\dot{Q}$ . One of the parameters most widely used to analyze the thermal behaviour of the pulsating heat pipes is its thermal resistance, which can be defined as:

$$R_{th} = \frac{\bar{T}_e - \bar{T}_c}{\dot{Q}} \quad (1)$$

where  $\bar{T}_e$  and  $\bar{T}_c$  are, respectively, the evaporator and the condenser mean temperatures ( $\bar{T}_e = \sum_{i=1}^8 Te_i / 8$ ;  $\bar{T}_c = \sum_{i=1}^6 Tc_i / 6$ ), both averaged over the successive recordings selected for the steady-state characterization.  $\dot{Q}$  is the overall heat power applied, not considering the heat losses due to the difficulty to identify them in such conditions.

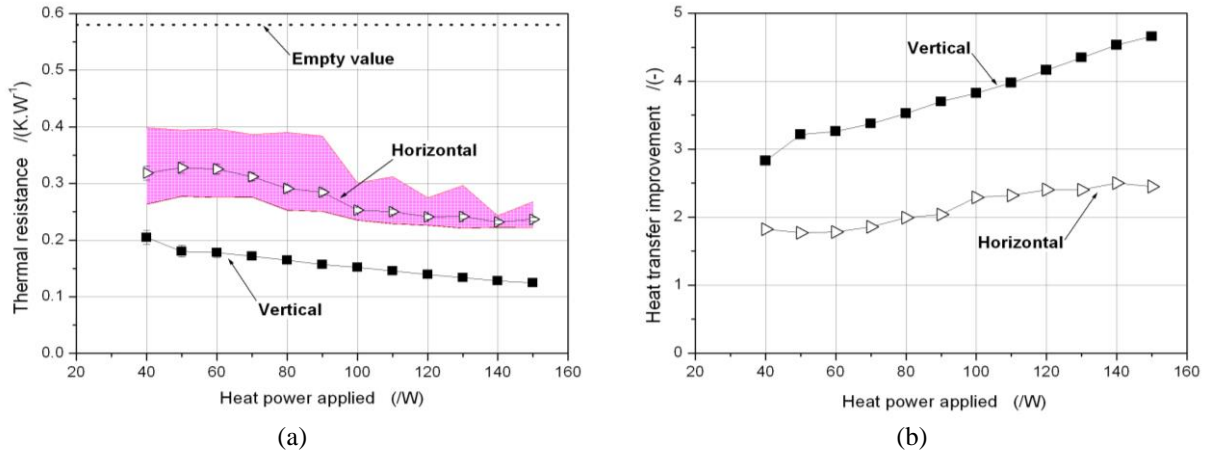


Fig. 7: (a) Thermal resistance and (b) Heat transfer improvement vs. heat power for the two orientations on ground.

Fig. 7a presents the FPPHP thermal resistance  $R_{th}$  as a function of heat power applied for both inclinations with corresponding error bars for each measurement, calculated using the measurement errors of temperatures and electric power acquisition system that affect the values of  $R_{th}$ . For vertical orientation, as already often observed in the literature for this configuration, the resistance curve is a smooth decreasing function of  $\dot{Q}$ . In horizontal inclination, the trend is less clearly delineated, but  $R_{th}$  likewise decreases, albeit less regularly than in vertical inclination, when increasing heat power is applied. The pink area surrounding the horizontal resistance curve represents the maximal and minimal resistance curves obtained from minimal and maximal evaporator temperatures, as measured based on the amplitude of the temperature fluctuations. Quite obviously, these boundaries have no actual physical meaning since the amplitude of the fluctuations depends on the stop-and-start fluid motion phenomena recorded during these highly specific tests. That said, for each power step it is helpful to have a snapshot of the influence of temperature fluctuations on thermal resistance

value. The influence area of these fluctuations is observably much greater than that of measurement error. The heat leaks, which usually increase with the temperature, i.e. the heating power, could motivate part of the decrease of thermal resistance, but no quantitative estimation can be given with the present tests. The variations of -22% and -42% for horizontal and vertical orientation respectively and the difference created by raising the power from 40 W to 150 W are in any case much greater than the possible relative effective heat variations due to leaks, and vertical orientation clearly leads to better and more continuous thermal performances than does horizontal orientation.

On Fig. 7a the dashed line corresponds to the resistance value of the empty FPPHP,  $R_{th,empty}$  (evaluated both from tests without fluid and from FEA numerical calculations carried out with StarCCM+). This value was calculated at 0.58 K/W. Fig. 7b presents the corresponding heat transfer improvement of the filled compared to the empty FPPHP,  $(1/R_{th})/(1/R_{th,empty})$ . It shows that heat transfer is further enhanced when more heating power is applied, and that while it is around twice the empty PHP for horizontal inclination, it grows from 2.8 times (at 40 W) to more than 4.5 times (at 150 W) in vertical orientation, thereby highlighting the satisfactory performances of these kinds of thermal systems.

### 3.2 Parabolic flight campaign

A parabolic flight campaign consists of three days of tests during which 31 parabolic trajectories are carried out every day, through six series of five consecutive parabolas with a five-minute break between each series [24]. In Fig. 8a the grey lines show the acceleration data along the z-axis (perpendicular to the floor of the plane) measured by the accelerometer during two parabolas. The fluctuations of these curves are due mainly to the vibrations of the support caused by the fans. The period of around 22 s of microgravity (with a nominal gravity of  $0.1 \text{ m}\cdot\text{s}^{-2}$ ) is preceded and followed by two periods of hypergravity (1.8g before and 1.6g after, approximately) of around 20 s each. These phases may affect the passage from one flow pattern to the other, and in order to compare the transient response of the FPPHP during a parabola to the FPPHP tested on the ground under the same conditions, a vertical-horizontal-vertical tilting manoeuvre simulating one parabola was carried out, as shown in Fig. 8b. The tests on the ground distinguish the transient responses of the FPPHP with microgravity from the responses presenting horizontal inclination. One may observe the effect of the hypergravity phases compared to normal ones on the ground, which may perturb the operation of the system from one configuration to another during transient phases. During parabolic



flights, the experiments were carried on in vertical orientation (bottom heated mode) with increasing heat power steps from 30 W up to 180 W for the first day, in horizontal inclination with the same increasing heat power steps (30 W) for the second day, and again in vertical position, with decreasing heat power steps from 180 W down to 30 W for the third day for repeatability purposes.

### 3.2.1 Tests in vertical orientation

Fig. 8 presents comparisons between temperature transient responses of the FPPHP recorded during one parabola (with two different heat power levels) and the same tests performed on ground simulating the parabolas by simply tilting the PHP from vertical to horizontal to vertical orientations with the same time periods as during a parabola, and following the same approach as Mameli and al. during their PF experiments [13]. As mentioned above, these manoeuvres are visible on the grey curves of acceleration along the  $z$ -axis of Fig. 8. Since the major goal of this experimental campaign is to determine whether there are differences in FPPHP thermal and hydraulic behaviour between ground-horizontal and microgravity environment operations, these ground tests were performed during the parabolic flights for all heat power levels.

Through comparison of the thermal transient responses of Fig. 8 between parabolic flight and simulated transient ground tests, it became evident that the FPPHP operation is less repeatable in horizontal or microgravity conditions than in the observations of Mameli et al. [13]. As highlighted in Fig. 5, due to a higher channel diameter FPPHP temperatures fluctuate much more under the above-mentioned operative conditions. In fact, since larger diameters result in smaller viscous losses and in a lower capillary pressure difference between the advancing and receding fronts of liquid slugs, the fluid inside the FPPHP is much quicker to respond to the configuration changes (vertical to horizontal or microgravity), which means that a nearly complete alteration of the thermo-hydraulic regime during the 22 s of microgravity may be observed.

In Fig. 5 it was shown that temperature fluctuations are much greater with low applied heat power. Finally, the higher  $\dot{Q}$ , the less fluctuating the FPPHP. Temperatures consequently show better repeatability and closer correspondence between PF and ground simulation tests for higher values of  $\dot{Q}$  (at  $\dot{Q} = 150$  W compared to  $\dot{Q} = 90$  W) in Fig. 8. This trend is even more pronounced when the applied heat power is high ( $\dot{Q} = 180$  W, Fig. 9a). Furthermore,

periods of hyper-gravity do not seem to affect the behaviour of the FPPHP in vertical orientation.

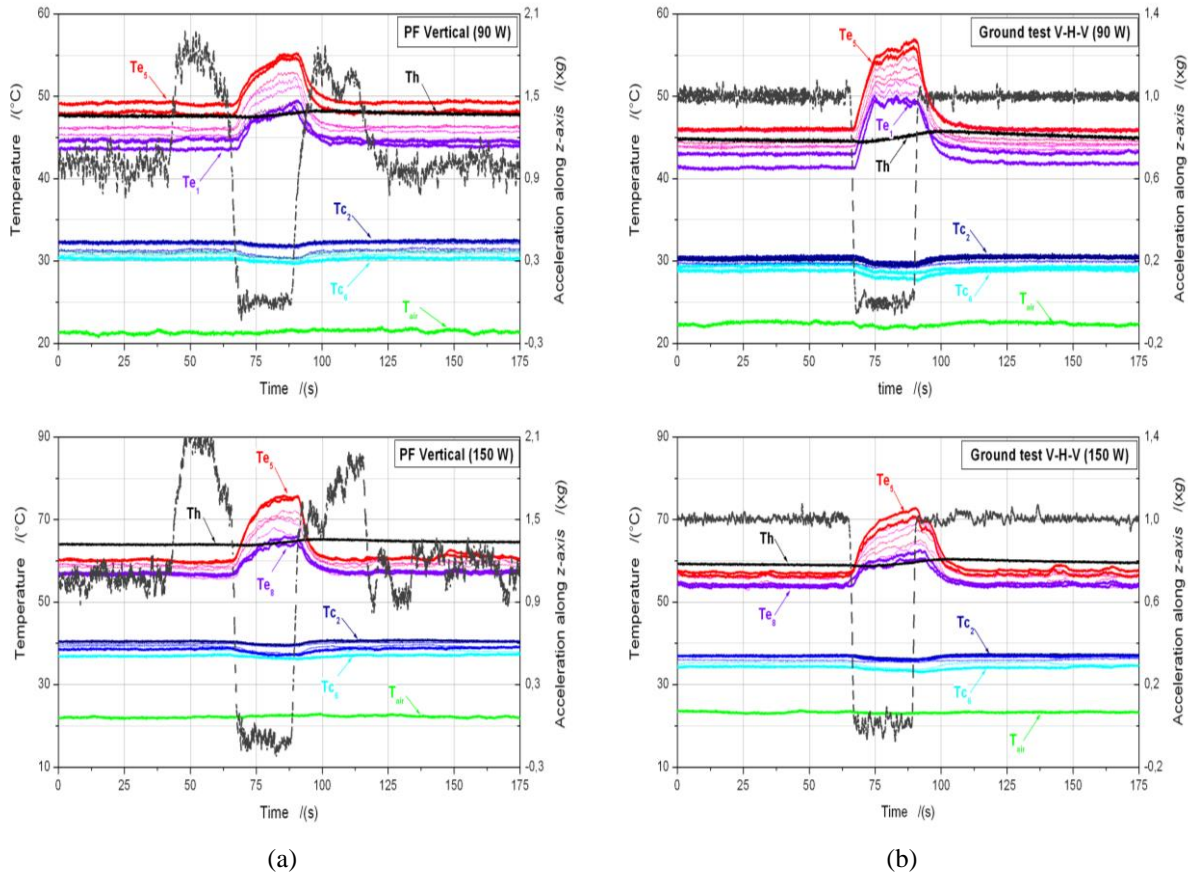


Fig. 8: FPPHP tested in vertical orientation at 90 W and 150 W: comparison between (a) parabolic flight (PF) and (b) ground tests (Ground test V-H-V) experiments.

Concerning the parabolic flight tests in vertical orientation, Fig. 9 shows representative profiles for the temperatures (Fig. 9a) and pressure (Fig. 9b) of the FPPHP for three values of heat power applied (30, 120 and 180 W) and two successive parabolas that highlight the effects of  $\dot{Q}$  on reproducibility. Regarding evaporator temperatures, they once again increase (see Fig. 8) during the microgravity period, because the fluid motion is no longer assisted by gravity [13]. Interestingly, the temperature increase can be very sharp, as is the case in the second parabola of Fig. 9a for 120 W heat power applied, and is accompanied by an equally rapid return to operation: the hydraulic response time of the flat plate pulsating heat pipe proves to be very short, lasting only a few seconds (between 5 s and 12 s according to the cases), while the fluid is in motion. Afterwards, as mentioned above, very different behaviour is observed in two successive parabolas for 30 W: at the second parabola, the FPPHP is immediately activated, and the temperature increase is visibly less pronounced. For increasing heat power levels, the dynamic temperature responses are more and more repeatable without a visible difference from one parabola to the next.

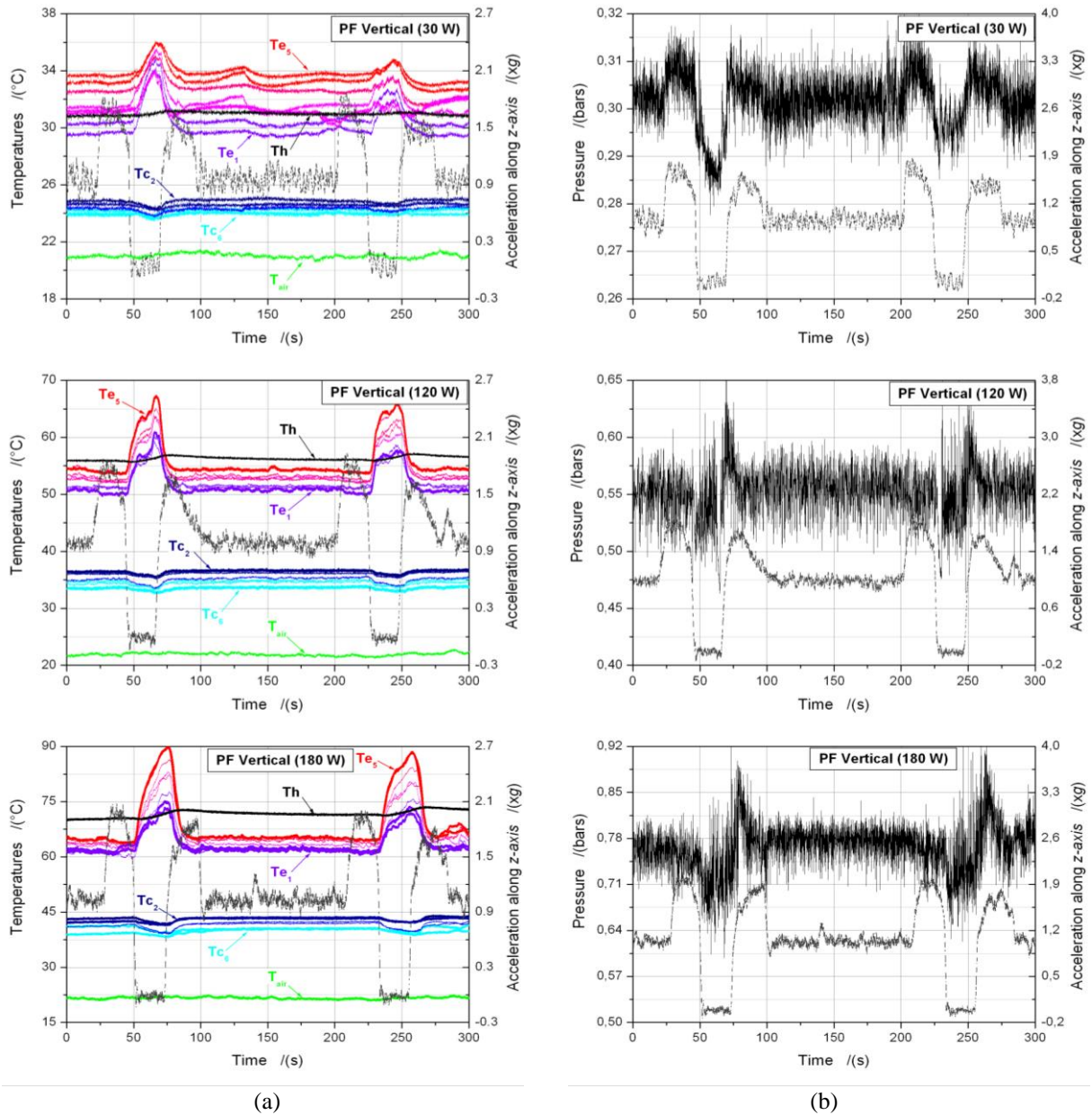


Fig. 9: Transient response of the FPPHP subject to two successive parabolic trajectories in vertical orientation: (a) temperatures; (b) pressure.

Since the pressure sensor is located in the highest section of the FPPHP in the condenser zone, it is therefore connected to the coldest FPPHP area. At 30 W, while the temperature signals are not affected during the hyper-gravity period, it is evident that a pressure increase occurs (of approximately 600 Pa, while noting that the overall gravity pressure drop for the liquid phase potentially approximates 2700 Pa over the entire height of the PHP). Knowing that, during this gravity transition, no change in the saturation temperature is detected, the pressure increase is therefore due to a change in either the hydraulic regime or in the fluid distribution in the tubes. What we do not know is whether the pressure increase is due to gravity pressure drop of some of the liquid plugs, which are

actually absent at higher heat power levels. At 30 W, during the starting parabola, most of the liquid is collected in the evaporator, and it oscillates slightly. During the hypergravity period the gravity force increases and a small difference of head between two close channels suffices to promote the short circulation of liquid slugs in the condenser along with a global pressure increases. In addition, during the first hypergravity phase a small temperature reduction has been observed.

The question arises because, in a previous parabolic flight experiment (CNES PF98, [23]), performed with another FPPHP developed for visualizations (the same apparatus as in [17]), it was observed that, for strictly annular flow patterns, an increase of gravity is accompanied by a slight decrease of temperatures at the evaporator. This may be explained by considering the thinning of the liquid film with increased gravity, leading to better heat transfer coefficient by conduction through the liquid film. Or else, in the case of liquid slugs accumulated in the evaporator, a gravity pressure drop between two liquid levels in two adjacent channels could suffice to promote liquid motion in hypergravity phase as compared to normal gravity. For the highest heat power levels, a *very* slight reduction in temperature at evaporator can also be observed on Fig. 9a, partially confirming previous evaluations.

The mean pressure level always decreases when passing from hyper to microgravity (Fig. 9b). When the temperature levels increase at the evaporator, they decrease at the condenser (Fig. 9a). Fluctuation amplitudes also increase during microgravity phases. This is confirmed by the difference of pressure fluctuation levels for vertical and horizontal ground experiments shown in Fig. 6. Pressure evolutions over time are highly affected by the mean temperature of the fluid inside the condenser and by the operative modes of the FPPHP. Gravity influences the amplitude oscillations of the slugs and plugs inside the FPPHP channels. Gravity usually enhances heat transfer and helps the condenser to keep the mean temperature value at a lower level. Analysing the results shown on Fig. 9b, it appears that the mean pressure value during 1g operation increases with input power, as does the condenser temperature, while decreases during the 0g period. In this period the effect of gravity on the circulation of the fluid is suspended and circulation is similar to horizontal case on ground with higher amplitude and lower frequency oscillations.

Finally, the transitions from microgravity to hyper-gravity (first case) are accompanied by an increase of the mean pressure, contrary to what happens in transitions from normal to hyper-gravity (second case), except at 30 W. This could be due to a change of flow pattern in

the first case (from slug flow to annular), together with an increase of condenser temperatures, which does not occur in the second case (only annular or semi-annular flow).

### 3.2.2 Tests in horizontal orientation

Tests in horizontal orientation are very important during parabolic flight experiments, because they help to determine whether gravity has an influence on the phase distribution, and consequently on flow patterns and heat and mass transfers: does there exist an influence of the gravity vector normal to channel direction on the shape of the menisci? If so, does it affect the possibility of maintaining a slug-and-plug regime? Can we imagine better performances with higher hydraulic diameters leading to very low pressure losses and maintaining liquid/vapour phase separation due to capillary forces? Operation of the horizontal FPPHP is not markedly influenced by a change in gravity levels (Fig. 10). When the hydraulic diameter is in the transition range for the static Bond number condition, capillarity in the channel corners could improve suction for smaller tube internal diameters. To verify this point, experiments with similar PHP geometry containing a circular section of the channel will help to understand the respective weight of the two effects, i.e. global capillary flow *vs.* wedge capillary entrainment.

At the lowest heat power (30 W) fluctuations are naturally very large, even for a fixed gravity field (Fig. 5). The top-left curves in Fig. 10a show that while some start-and-stop phases are noticeable and correspond to gravity changes (first parabola), others also occur during the following constant 1g periods, and are not particularly affected during the transitions (second parabola). Therefore, the temperature instabilities observed for horizontal inclination are primarily a result not of the change in gravity levels, but rather of the low thermal drive.

This phenomenon is even more pronounced when heat power is high. If some instabilities are still noticeable for 120 W (for temperature and pressure signals), no significant change is visible during the transition phases for 180 W.

Analysis of the results on Fig. 10b shows that, for higher input powers, no change is observed between the transition from normal gravity to microgravity and *vice versa*. The effect of gravity is not evident in these test cases because a PHP operates in a microgravity environment as well as on ground, at horizontal orientation. For low input powers, where nearly no circulation / low amplitude oscillations are likely to occur in the FPPHP, the effect of gravity reduction is more random and can promote random oscillations inside the channels. This could explain the random behaviour observed at 30W in Fig. 10b.

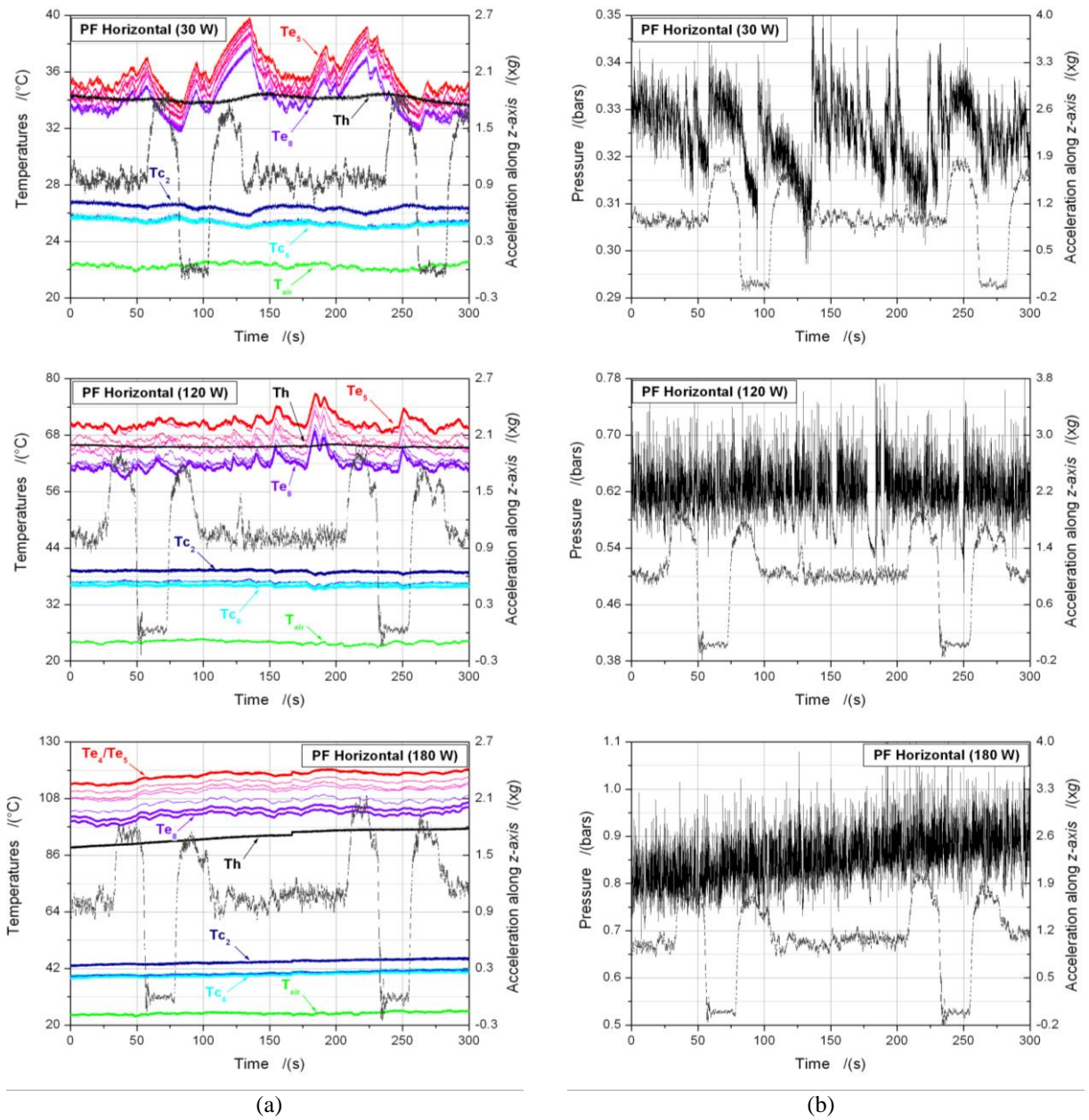


Fig. 10: Transient response of the FPPHP subject to two successive parabolic trajectories (horizontal orientation): (a) temperatures; (b) pressure.

One can therefore assume that when tilted horizontally a flat plate pulsating heat pipe can operate similarly under microgravity to the way it does on the ground. This is a significant result because it once again shows that, despite some persisting issues related to redundancy, pulsating heat pipes are a promising technology for space applications. It would be essential to test such systems with tube diameters larger than the 1g capillary diameter in order to be able to achieve operational goals having to do with space application.

Finally, it is worthwhile to underline that no evaluation of the thermal resistances during the parabolic flight, i.e. during an instationary regime, can be given, since thermal resistance can be calculated only for steady state conditions. A rough comparison of the

FPPHP performances on the ground and for the different gravity levels may be inferred looking at maximum evaporator temperatures.

## Conclusions

A Closed Loop Flat Plate Pulsating Heat Pipe (FPPHP) has been tested on ground and in hyper- and micro-gravity conditions during the 60<sup>th</sup> ESA parabolic flight campaign. The purpose was to test an innovative FPPHP, which behaves differently from tubular PHPs due to two main characteristics: (i) the square/rectangular channels with sharp angles and (ii) the transverse heat spreading throughout the continuity of the plate bulk. The latter effect has been partially smoothed thanks to the novel insertion of separating grooves limiting transverse conductive heat flux. The tests showed that the system was also operational in horizontal orientation, with good performances (more than twice the void PHP equivalent thermal conduction). Furthermore, using a pressure sensor in the device linked temperature variations to hydraulic flow pattern changes, particularly from one gravity configuration to another (horizontal/vertical, hyper/microgravity transitions). The main observations to be drawn from this set of results are:

- The FPPHP works more effectively for ground tests in bottom heated vertical than in horizontal orientation. Pressure fluctuations and thermal instabilities are greater in horizontal position, with stop-and-start phases that decrease with increasing heat power.
- Compared to the tubular PHP tested by Mameli and al. [13], this FPPHP has proved to be quicker to respond to gravity variations in horizontal inclination, mainly on account of the higher hydraulic diameter of its channels: the experiments conducted during parabolic flight and on ground simulating the transition from vertical to horizontal orientation showed similar transient behaviour, with a steady-state regime reached in only 22 s of microgravity, at least from a hydraulic point of view. It demonstrates that the system is very quick to respond to transient changes.
- The thermal behaviour of the pulsating heat pipe tested in the vertical orientation is obviously influenced by the change of gravity levels, due to distinct thermal performances markedly varying from one case to the other. The occurrence of annular flow patterns is (most) probably the cause of such behaviour, compared to slug flow patterns in horizontal orientation or under microgravity conditions.

- The more the heat power level increases, the more stable and efficient the PHP, showing reproducible behaviour for parabolas performed for the highest  $\dot{Q}$  values.
- The FPPHP tested in horizontal inclination is not influenced by changes of gravity levels, proving that such a system can be an efficient candidate for thermal control in different space applications, once a greater channel size is combined with a sufficient number of turns.
- The effect of the “wedge-capillary” due to the rectangular shape of the channels should be further investigated.

## Acknowledgments

The authors acknowledge the financial support of the Italian Space Agency through the ASI-AO2009 DOLFIN-II within the ESA 60<sup>th</sup> parabolic flight campaign. Special thanks must be given to NOVESPACE team in Bordeaux for their assistance in developing the experimental setup, and to Dr. Vladimir Pletser from ESA for his support in the PF campaign. Lastly, let us not forget Dr. Olivier Minster and Dr. Balazs Toth in the acknowledgements for their interest and support to the PHP research activities. An American translator, Jeffrey Arsham, reviewed and revised our original English-language manuscript.

## References

- [1] H. Akachi, Structure of a heat pipe, US Patent No. 4921041, 1990.
- [2] B. Tong, T. Wong, K. Ooi, Closed-loop pulsating heat pipe, *Appl. Therm. Eng.* 21 (2001) 1845-1862.
- [3] S. Khandekar, P. Charoensawan, M. Groll, P. Terdtoon, Closed loop pulsating heat pipes, Part B: visualization and semi-empirical modeling, *Appl. Thermal Eng.* 23 (2003) 2021-2033.
- [4] S. Liu, J. Li, X. Dong, H. Chen, Experimental study of flow patterns and improved configurations for pulsating heat pipes, *J. of Therm. Sc.* 16 (2007) 56-62.
- [5] S. Khandekar, N. Dollinger, M. Groll, Understanding operational regimes of closed pulsating heat pipes: an experimental study, *Appl. Therm. Eng.* 23 (2003) 707-719.
- [6] P. Charoensawan, S. Khandekar, M. Groll, P. Terdtoon, Closed loop pulsating heat pipes, Part A: parametric experimental investigations, *Appl. Therm. Eng.* 23 (2003) 2009-2020.
- [7] S. Liu, X. Dong, H. Chen, Experimental study of flow patterns and improved configurations for pulsating heat pipes, *J. of Therm. Sc.* 16 (2006) 56-62.
- [8] H. Yang, S. Khandekar, M. Groll, Operational limit of closed loop pulsating heat pipes, *Appl. Therm. Eng.* 28(1) (2008) 49-59.



- [9] V. Ayel, Y. Bertin, C. Romestant, G. Burban, Experimental study of pulsating heat pipes tested in horizontal and vertical positions, Proc. Of 15<sup>th</sup> Int. Heat Pipe Conf. (15<sup>th</sup> IHPC), Clemson, USA, April 25-30, 2010.
- [10] M. Mameli, M. Marengo, S. Filippeschi, V. Manno, Multi-parametric investigation on the thermal instability of a closed loop pulsating heat pipe, Proc. Of 17<sup>th</sup> Int. Heat Pipe Conf. (17<sup>th</sup> IHPC), Kanpur, India, October 13-17, 2013.
- [11] S. Khandekar, M. Groll, P. Charoensawan, S. Rittidech, P. Terdtoon, Closed and open loop pulsating heat pipes, 13<sup>th</sup> Int. Heat Pipe Conference (13<sup>th</sup> IHPC), Shanghai, China, Sept. 21-25, 2004.
- [12] J-F Bonnenfant, Y. Bertin, V. Ayel, C. Romestant, Experimental study of pulsating heat pipes tested in looped and unlooped configurations, 16<sup>th</sup> Int. Heat Pipe Conference (16<sup>th</sup> IHPC), Lyon, France, May 20-24, 2012.
- [13] M. Mameli, L. Araneo, S. Filippeschi, L. Marelli, R. Testa, M. Marengo, Thermal response of a closed loop pulsating heat pipe under a varying gravity force, Int. J. Therm. Sc. 80 (2014) 11-22.
- [14] J. Gu, M. Kawaji, R. Futamata, Effects of gravity on the performances of pulsating heat pipes, J. Thermophys. Heat Transf. 18(3) (2004) 370-378.
- [15] S. Khandekar, M. Schneider, P. Schäfer, R. Kulenovic, M. Groll, Thermofluid dynamic study of flat-plate closed-loop pulsating heat pipes, Microscale Thermophys. Eng. 6 (2002) 303-317.
- [16] H. Yang, S. Khandekar, M. Groll, Performance characteristics of pulsating heat pipes as integral thermal spreaders, Int. J. Therm. Sc. 48 (2009) 815-824.
- [17] V. Ayel, C. Romestant, Y. Bertin, V. Manno, S. Filippeschi, Visualisation of flow patterns in flat plate pulsating heat pipe: influence of hydraulic behaviour on thermal performances, Proc. Of 17<sup>th</sup> Int. Heat Pipe Conf. (17<sup>th</sup> IHPC), Kanpur, India, October 13-17, 2013.
- [18] J. Qu, H. Wu, P. Cheng, Start-up, heat transfer and flow characteristics of silicon-based micro pulsating heat pipes, Int. J. Heat Mass Tr. 55 (2012) 6109-6120.
- [19] C. Baldassarri, M. Marengo, Flow boiling in microchannels and microgravity, Prog. Energy Combust. Sc. 39 (2013) 1-36.
- [20] J. Gu, M. Kawaji, R. Futamata, Microgravity performance of micro pulsating heat pipe, Microgravity Sci. Technol. 16 (2005) 181-185.
- [21] C.D. Henry, J. Kim, B. Chamberlain, Heater Size and Heater aspect ratio effects on subcooled pool boiling heat transfer in low-g, 3rd int. Symposium on two phase flow modeling and experimentation, Pisa 22-24 September 2004.
- [22] X. Liu, Y. Chen, M. Shi, Dynamic performance analysis on start-up of closed loop pulsating heat pipes (CLPHPs), Int. J. Therm. Sc. 65 (2013) 224-233.
- [23] V. Ayel, F. Thévenot, C. Romestant, Y. Bertin, Analyse thermo-hydraulique expérimentale d'un caloduc oscillant sous champ de gravité variable, Proc. Of Congrès Français de Thermique (SFT 2013), Gérardmer, France, May 28-31, 2013.
- [24] Novespace A300 Zero-g Rules and Guidelines, April, 7<sup>th</sup>2009. RG-2009-2, NOVESPACE, 15, rue des Halles, 75001 Paris, France.